



# Time is a stronger predictor of microbiome community composition than tissue in external mucosal surfaces of Atlantic salmon (*Salmo salar*) reared in a semi-natural freshwater environment

Marlene Lorgen-Ritchie<sup>a</sup>, Lynn Chalmers<sup>b</sup>, Michael Clarkson<sup>b</sup>, John F. Taylor<sup>b</sup>,  
Herve Migaud<sup>b</sup>, Samuel A.M. Martin<sup>a,\*</sup>

<sup>a</sup> Scottish Fish Immunology Research Centre, School of Biological Sciences, University of Aberdeen, Aberdeen AB24 2TZ, UK

<sup>b</sup> Institute of Aquaculture, University of Stirling, Stirling FK9 4LA, UK

## ARTICLE INFO

### Keywords:

Aquaculture  
Atlantic salmon  
Microbiome  
Mucosal surfaces  
Temporal dynamics

## ABSTRACT

The mucosal surfaces provide the first line of defence to opportunistic pathogens in the external environment as well as other physiological functions including osmoregulation, gas exchange or nutrient absorption in the gut. Atlantic salmon is the most valuable salmonid species cultured worldwide and its anadromous life cycle dictates periods of growth in both fresh and seawater. The transition of fish between these two habitats is often accompanied by high levels of mortality. Communities of commensal microbes inhabiting mucosal surfaces are vital in fish health and are also subjected to an abrupt change in salinity and often temperature during seawater transfer of Atlantic salmon. In this study we followed a cohort of Atlantic salmon through parr-smolt transformation in an open freshwater loch exposed to a natural decline in water temperature and during the first month post-transfer to sea. Mucus swabs were taken from gill and skin, and hindgut were collected from  $n = 6$  fish from triplicate pens at four sampling points in freshwater (FW) and in the first- and fourth-weeks post transfer to sea ( $n = 18$  total per sampling). Distinct temporal dynamics and communities were identified in the three mucosal surfaces. The hindgut microbiome diversity was stable and characterized by high inter-individual variability in terms of community composition. Microbiome diversity decreased in the skin throughout FW rearing and immediately post-transfer to sea but recovered to pre-transfer levels after one month at sea. Gill microbiome diversity also declined post-transfer but continued to decline further due to a single dominant taxon identified as *Candidatus Clavichlamydia salmonicola*, a member of the phylum *Chlamydiae*. Mucosal microbiome communities in all surfaces were largely distinct from the surrounding water. This study highlights the importance of considering the impact of time, in conjunction with water temperature and salinity, when determining microbiome composition in fish and urges caution when inferring general functionality of the microbiome from a single time point.

## 1. Introduction

As the world population continues to expand, so too does the need to produce sufficient high-quality protein to meet the UN sustainable development goal number two – ‘zero hunger’. Aquaculture is a key sector in meeting this target with global aquaculture production of aquatic animals reaching 87.5 million tonnes in 2020 and accounting for 56% of production for human consumption (FAO, 2022). Atlantic salmon (*Salmo salar* L.) is the most valuable finfish farmed worldwide (FAO, 2020). Farming of Atlantic salmon is complex due to the

anadromous life cycle that dictates an early period of growth in freshwater (FW) followed by on growing in seawater (SW). To enable this transfer between salinities, juveniles undergo many physiological, morphological and behavioural changes known collectively as parr-smolt transformation (PST) in FW to preadapt to the osmoregulatory shift experienced when transferred to sea (McCormick, 2012). Seawater transfer (SWT) is a period associated with high levels of mortality (Khaw et al., 2021). The production of robust seawater tolerant smolts is critical for fish welfare and performance at sea and this remains a challenge for the industry. Smolts can be reared in open water (e.g. lochs in Scotland)

\* Corresponding author.

E-mail address: [sam.martin@abdn.ac.uk](mailto:sam.martin@abdn.ac.uk) (S.A.M. Martin).

<https://doi.org/10.1016/j.aquaculture.2022.739211>

Received 2 August 2022; Received in revised form 20 November 2022; Accepted 26 December 2022

Available online 28 December 2022

0044-8486/© 2022 The Authors. Published by Elsevier B.V. This is an open access article under the CC BY license (<http://creativecommons.org/licenses/by/4.0/>).

or land-based flow-through or recirculating aquaculture systems (RAS) and of particular interest in recent years has been how FW rearing history can impact fish susceptibility to disease and performance during on-growing in SW (Kolarevic et al., 2014).

Mucosal layers are the first line of defence against pathogens (Salinas et al., 2021). One component of fish health which is sensitive to the environment is the commensal communities of bacteria known as microbiomes which inhabit all mucosal surfaces of teleost fishes. Fish mucus contains an array of antimicrobial enzymes and peptides with protective immune roles (Gomez et al., 2013; Xu et al., 2016). Like mammals, the internal surface of the gut is covered by a mucus layer. Additionally, residing in an aquatic environment rich in potential microbial pathogens, teleosts also retain an ancestral vertebrate ability to produce an active protective mucus layer from goblet cells within the epidermis and gill arches, a function which was lost when vertebrates colonised land (Xu et al., 2013; Salinas et al., 2021). Additionally, teleost gill and skin play many important functions ranging from osmoregulation and ion balance to gas exchange and waste excretion (Glover et al., 2013). Importantly, the large surface areas and constant contact with surrounding microbe rich water make both gill and skin principal sites for host-pathogen interactions (Xu et al., 2016).

The microbiomes which inhabit mucosal surfaces have been well studied in Atlantic salmon, particularly in the gut, and findings demonstrated the impacts of environment (Uren Webster et al., 2020), diet (Zarkasi et al., 2016), life history stage (Llewellyn et al., 2016; Lokesh et al., 2019), SW transfer (Dehler et al., 2017), and the impact of time post-SWT (Wang et al., 2021). The study of external mucosal communities has gained increasing interest in recent years with relevance for the environment (Uren Webster et al., 2020), rearing systems (Minich et al., 2020a), sampling techniques (Clinton et al., 2021) and disease (Slinger et al., 2021; Brown et al., 2021). Studies incorporating more than one mucosal surface have been performed in different rearing systems used for Atlantic salmon farming including FW RAS system where environmental conditions are carefully managed (Minich et al., 2020a), flow-through SW system (Bledsoe et al., 2022) and also in wild populations (Uren Webster et al., 2018). However, to date, no comparative studies have been conducted in semi-natural open aquaculture environments commonly used in commercial aquaculture in Scotland. Additionally, previously published studies did not consider temporal changes. Microbiome composition was shown to vary over time with life cycle stage (Lokesh et al., 2019), seasonality (Zarkasi et al., 2014) and during FW rearing (Lorgen-Ritchie et al., 2021).

In the present study, we examined temporal dynamics of gill, skin and hindgut microbiomes in Atlantic salmon through the parr-smolt transformation in a commercial open loch facility and in the first month post-transfer to sea using 16S rRNA amplicon sequencing. We considered diversity and richness, community composition and also core microbiota in each tissue.

## 2. Materials and methods

### 2.1. Fish maintenance and sampling schedule

Mixed sex juvenile Atlantic salmon were sampled at multiple time-points at both parr and smolt stages in a FW open loch aquaculture system and following transfer to sea cages. The onset of parr-smolt transformation (PST) is determined by a combination of temperature and increasing daylength which is simulated in an aquaculture setting using a measure called degree days (dd), a cumulative temperature over a number of days where  $dd = 0$  denotes the onset of an artificial spring (increasing) photoperiod. Fish were first sampled at the parr stage at  $-904$  dd (FW1 – 13th August 2019). Fish were then vaccinated (ALPHA JECT micro® 6, Pharmaq) and graded, and three experimental pens of medium grade fish were established. Fish were exposed to a naturally declining photoperiod for 887 dd (10 weeks) and sampled at  $-458$  dd (FW2 – 12th September 2019) and  $-112$  dd (FW3 – 11th October 2019).

The final FW sampling (FW4 – 12th December 2019; 364 dd) was 4 days prior to SWT following application of a “spring” signal in the form of constant light (LL) for seven weeks. Fish were transferred at approximately 400 dd in the week beginning 16th December 2019 to a seawater cage site. Temperature ranged from  $16.8$  °C at initial sampling in FW to  $5.9$  °C at the final FW sampling. Fish were sampled twice in SW, one week (23rd December 2019) and four weeks (16th January 2020) post-SWT. At each sampling point in FW and SW, six fish were sampled from triplicate cages ( $n = 3$  cages, 18 fish in total per sampling). All dd represent mean values across replicate cages. Fish were fed commercial organic diets throughout (Ewos Harmony 40P (2.7 mm) from August to October / Ewos Harmony 80P (3.3 mm) from November). Fish were bath treated with bronopol (Cress,  $0.5$  g / mL) and formaldehyde ( $375$  mg / mL) in August and September. The experimental design is depicted in Fig. 1.

Fish were culled by lethal anaesthesia (MS-222,  $1$  mg / mL, PHAR-MAQ, Norway) before sampling. Weight (g) and fork length (cm) of all fish was recorded. Gill and skin samples were collected as previously described (Lorgen-Ritchie et al., 2022), as were hindgut, water and diet samples (Lorgen-Ritchie et al., 2021). Briefly, cotton swabs were rolled gently across all gill arches on the left side to collect gill mucus, and similarly, swabs were gently rolled along the left side lateral line to collect skin mucus. All swabs were placed in 2 mL sample collection tubes containing 1.5 mL RNAlater™ (Ambion Inc., USA). Hindgut samples were also collected in 1.5 mL RNAlater™ following aseptic dissection of the hindgut along with any digesta ( $100$ – $150$  mg of tissue). All samples were kept at  $4$  °C for 24 h to allow RNAlater™ to permeate prior to longer term storage at  $-80$  °C. At each sampling point, cage water samples ( $4 \times 50$  mL) were also collected and transferred to the lab at room temperature prior to storage at  $-20$  °C. Water samples were filtered through  $0.2$  µm Whatman Cyclopure polycarbonate membrane filters (Sigma-Aldrich; WHA70634702) using a vacuum pump and filters stored at  $-80$  °C until DNA extraction. Diet samples were collected at the final FW sampling point and both SW sampling points, transferred to the lab at room temperature and stored at  $-80$  °C until DNA extraction.

Heparinised syringes were used to collect blood. Blood samples were then centrifuged ( $2500$ RPM at  $4$  °C for 15 min) to separate plasma for chloride analyses which was stored at  $-20$  °C. For  $\text{Na}^+$ ,  $\text{K}^+$  – ATPase (NKA) enzyme activity analysis a total of 4–6 gill filaments from the primary gill arch were collected in SEI buffer ( $150$  mM sucrose,  $10$  mM EDTA,  $50$  mM imidazole, pH 7.3) and flash frozen on liquid nitrogen. Temperature data was obtained from routine recording.

### 2.2. Parr-smolt transformation assessments

At each FW sampling, smolt index was determined using the following scale: 1, parr; 2, some silvering, parr marks visible; 3, fully silvered, but parr marks visible; 4, smolt, no parr marks visible (Sigholt et al., 1995). Colorimetric titration was used to determine plasma chloride ( $\text{Cl}^-$ ) according to manufacturer's protocol using silver nitrate as the reagent (926S Chloride Analyser, Sherwood Scientific, Cambridge).  $\text{Na}^+$ ,  $\text{K}^+$  – ATPase activity was assessed at Stirling University with a kinetic assay run at  $26$  °C and read at a wavelength of  $340$  nm for 10 min in 96-well microplates according to (McCormick, 1993).  $\text{Na}^+$ ,  $\text{K}^+$  – ATPase protein concentrations were determined using a BCA (Bicinchoninic acid) Protein assay kit (SIGMA, Aldrich, UK).

### 2.3. DNA extraction

Samples were prepared for DNA extraction as described previously (Lorgen-Ritchie et al., 2021; Lorgen-Ritchie et al., 2022). Briefly, on ice, mucus swabs were thawed and a scalpel was used to cut the swab in half lengthwise. The swabs were squeezed with tissue to remove excess RNAlater™. Hindgut samples were also thawed on ice and a scalpel used to slice the tissue open lengthwise and scrape out  $50$  mg (maximum) of digesta and internal mucosa. Hindgut samples were also squeezed with

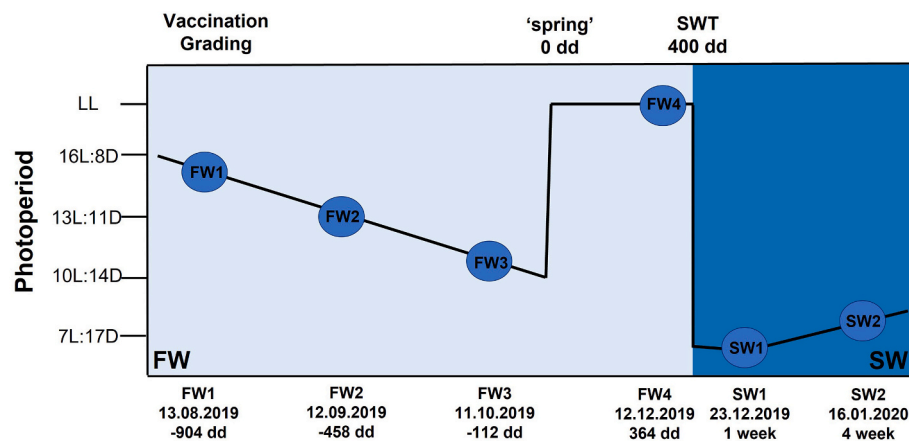


**Fig. 1.** Experimental design for microbiome sampling at open FW and SW lochs. Blue circles represent sampling points; four in FW and two in SW. Degree days (dd) is a measure used to determine smolt windows. All dd are calculated relative to application of spring photoperiod (0 dd). Fish were first sampled at -904 dd (FW1), prior to vaccination and grading. Fish were then vaccinated and graded and three cages of medium grade fish were followed across exposure to a naturally declining photoperiod for 887 dd and sampled at -458 dd (FW2) and -112 dd (FW3). “Spring” photoperiod (24 h light – LL) was then applied for 7 weeks until SWT and fish were sampled at 364 dd (FW4) prior to SWT at approximately 400 dd. Fish in open SW cages sampled at approximately 1 and 4 weeks post-SWT. At all sampling points, six fish were sampled from triplicate cages ( $n = 3$ , 18 fish in total per sampling). (For interpretation of the references to colour in this figure legend, the reader is referred to the web version of this article.)

tissue to remove excess salt storage solution. The QIAamp Fast DNA Stool Mini Kit (Qiagen) was used for DNA extraction according to the manufacturers protocol with the addition of modifications described in (Dehler et al., 2017). Briefly, two 3 mm tungsten carbide beads (Qiagen) were added to a 2 mL Eppendorf tube containing a sample and InhibitEx buffer. Samples were pre-treated using a TissueLyser to mechanically lyse the samples for a total of 4 min. A final elution volume of 30  $\mu$ L was obtained. Care was taken to ensure that each batch of extractions contained samples from all across timepoints and tissues to protect against technical artefacts and each batch also included a negative extraction control. The same protocol was used to extract DNA from water filters and triplicate diet samples using 100 mg of pellets in each replicate.

#### 2.4. PCR amplification and sequencing

PCR reactions and subsequent library preparations were carried out as previously described (Lorgen-Ritchie et al., 2021). Variable regions 3 and 4 of the 16S rRNA gene were targeted for PCR amplification with the 341F/785R primer pair (Klindworth et al., 2013) with added Illumina adapter overhang sequences on 5' end of each primer. The sequence of the forward primer (341F) was 5' TCGTCGGCAGCGTCAGATGTGTA-TAAGAGACAGCCTACGGGNGGGCWCAG, and the reverse primer (785R) was 5' GTCTCGTGGCTCGGAGATGTGTATAAGAGACAGGACTA CHVGGTATCTAATCC. The bold sequences are the locus-specific V3–V4 primers and the remaining sequence the overhangs. In short, PCR reactions were performed in triplicate 10  $\mu$ L reactions with 2  $\mu$ L of each primer (1  $\mu$ M stock, Sigma), 5  $\mu$ L of 2 $\times$  KAPA HiFi HotStart ReadyMix (KAPA Biosystems Ltd., UK) and 1  $\mu$ L of undiluted DNA. The PCR cycling programme consisted of initial denaturation at 95  $^{\circ}$ C for 3 min, followed by 27 cycles of 30 s at 98  $^{\circ}$ C, 30 s at 57  $^{\circ}$ C and 30 s at 72  $^{\circ}$ C with a final extension of 72  $^{\circ}$ C for 5 min. An Agilent 2200 TapeStation (Agilent Technologies, Italy) was used to check a subset of PCR reactions to verify amplification of a product of the correct size. To produce libraries, dual indices and illumine sequencing adapters (P5 and P7) were attached to amplicons using the Nextera XT Index Kit (Illumina, San Diego, CA). The Quant-iT High-Sensitivity dsDNA Assay (ThermoFisher, USA) was used to quantify libraries on an Omega FLUOstar plate reader (BMG Labtech, UK) to enable equimolar pooling. Prior to loading onto a MiSeq flow cell, the final library was denatured and diluted to a concentration of 1.2 nM. To obtain the desired sequencing depth, two flow cells were utilised with samples randomised between two libraries. Sequencing was performed using a 2  $\times$  300 bp paired end protocol on an Illumina MiSeq platform (Illumina, San Diego, CA).

#### 2.5. Sequencing data bioinformatics

Sequence data were analysed with DADA2 (Callahan et al., 2016) and Phyloseq (McMurdie and Holmes, 2013) in RStudio v1.1.456 as described previously (Lorgen-Ritchie et al., 2021). Briefly, TrimGalore! (<https://github.com/FelixKrueger/TrimGalore>) was used to remove adapters and primers from reads, and those with a Phred quality score of <30 were discarded. Reads were truncated to 250 bp (forward) or 200 bp (reverse) to remove poor quality ends and leave sufficient overlapping sequence for merging. Reads were then subjected to denoising, merging, screening for chimeric sequences (which were removed) and finally assignment as amplicon sequence variants (ASVs) using DADA2. Samples with low coverage (<1000 reads) were excluded from further analysis. Classification of ASVs at the taxonomic levels was conducted out using the assignTaxonomy function of DADA2 and the Silva reference taxonomy v132 (Quast et al., 2013). Taxonomic assignment at the species level was also carried out utilising the Silva species assignment v132 and allowing for the assignment of multiple species. To further identify ASVs of interest to species level, BLASTn searches were carried out against both the NCBI nucleotide collection and the rRNA/TTS databases. Hits were accepted only when sequence identity was at least 99.5% and cover of the sequence was 100%. Reads mapping to irrelevant products known to be co-amplified including eukaryotic, mitochondrial, chloroplast and cyanobacteria taxa were removed from analysis in addition to ASVs that were present as singletons. Following removal of co-amplified sequences, samples with <500 reads were discarded prior to further analysis. The community composition of the triplicate positive controls aligned with the mock community reference (Fig. S1).

#### 2.6. Statistical analysis

Statistical analyses were conducted in RStudio v1.1.456 using R v3.6.1 and phyloseq (McMurdie and Holmes, 2013) as described previously (Lorgen-Ritchie et al., 2021). One-way ANOVA with Tukey's HSD post-hoc test was used to analyse growth and PST parameters. Prior to assessing alpha and beta diversity, all samples were sub-sampled to an equal depth of 4604 reads to ensure comparable read depth while maintaining sample size across experimental groups. Kruskal-Wallis comparison of alpha diversity metrics including Shannon (Shannon, 1948) and Chao1 (Chao, 1984) across sampling points was conducted and followed up with the Wilcoxon rank sum test for pairwise testing.

Bray-Curtis dissimilarity distance (Bray and Curtis, 1957) was used to calculate beta diversity and community composition differences were visualized using non-metric multidimensional scaling (NMDS) ordination plots, created using the Vegan package (Oksanen et al., 2017) and

plotted with ggplot2 (Wickham, 2016). To present a visual summary, stat-ellipse in ggplot2 were used to draw data ellipses based upon an assumed multivariate t-distribution at a level of 0.75. The Adonis function within the Vegan package was used to conduct permutational multivariate statistical analysis of community separation (PERMANOVA) across sampling points in each tissue individually and across all tissues. Adonis.pair in the EcolUtils package (Salazar, 2020) was used to compute pairwise comparisons. The microbiome package (Lahti and Shetty, 2017) was used to identify core taxa employing a relative abundance threshold of 0.1% and a prevalence cut-off of 90%. Log<sub>2</sub> relative abundances of core ASVs across samples were presented in heatmaps drawn with Pheatmap (Kolde, 2012) which was used to produce heatmaps of log<sub>2</sub> relative abundances of core taxa across all samples, with distance clustering conducted using Euclidean distances.

### 3. Results

#### 3.1. Fish growth and condition factor

Fish length and weight increased significantly throughout sampling ( $p < 0.001$ ; Table 1) and condition factor showed a decline throughout FW ( $p < 0.001$ ), in line with PST. Prior to seawater transfer, the mean smolt index score was  $3.3 \pm 0.2$  and gill NKA activity was  $13.09 \pm 2.33 \mu\text{M mg prot}^{-1} \text{h}^{-1}$ , respectively. Both parameters indicated appropriate final smolt status prior to seawater transfer. Plasma chloride was significantly increased initially following transfer to SW before declining, but levels remained significantly higher than FW levels after four weeks in SW. No significant differences were identified in SGR between sampling periods and SGR across the entire study equated to 1.03% body weight per day.

#### 3.2. Sequencing outputs

From 108 fish, 5,149,061 raw reads were obtained from gill samples (mean read depth =  $47,676 \pm 4668$  (SE)), 4,935,017 from skin (mean =  $45,695 \pm 5321$ ) and 9,192,518 from hindgut (mean =  $85,116 \pm 7686$ ). After quality filtering, denoising and chimera removal in DADA2, 2,317,775 reads from gill samples (mean =  $21,461 \pm 2537$ ), 2,020,064 from skin (mean =  $18,704 \pm 2410$ ) and 4,650,333 reads (mean =  $43,059 \pm 4113$ ) from hindgut. All 108 gill samples were retained for downstream analysis while 104 skin and 105 hindgut samples were retained.

#### 3.3. Alpha diversity

Gill. Diversity (Shannon  $F = 53.2$ ,  $p < 0.001$ ; Fig. 2 A1) and richness (Chao1  $F = 48.2$ ,  $p < 0.001$ ; Fig. 2 B1) changed significantly over time in

gill. In the FW phase, no significant differences were identified between sampling points. During SWT (FW4 to SW1), diversity showed a significant and stepwise temporal decline ( $p < 0.001$ ) to SW2. Richness also declined from FW4 to SW1 ( $p < 0.001$ ) but remained constant from SW1 to SW2.

Skin. Diversity (Shannon  $F = 53.5$ ,  $p < 0.001$ ; Fig. 2 A2) and richness (Chao1  $F = 29.6$ ,  $p < 0.001$ ; Fig. 2 B2) were modulated over time in skin. In the FW phase, pairwise analysis revealed significantly higher diversity at FW1 when compared to FW3 ( $p < 0.05$ ) or FW4 ( $p < 0.001$ ), at FW2 when compared to FW3 and FW4 ( $p < 0.001$ ), and at FW3 when compared to FW4 (all at  $p < 0.01$ ). Species richness was also significantly higher at FW2 compared to FW3 ( $p < 0.05$ ) and FW4 ( $p < 0.01$ ). As in the gill, during SWT, both diversity ( $p < 0.01$ ) and richness ( $p < 0.001$ ) showed significant declines. In contrast with gill, diversity ( $p < 0.001$ ) increased from SW1 to SW2, recovering to pre-transfer (FW3 and FW4) levels.

Hindgut. Alpha diversity metrics Shannon and Chao1 indicated low diversity and richness in hindgut in both fresh and seawater. No significant temporal changes were identified in diversity (Fig. 2 A3) or richness (Fig. 2 B3) in hindgut.

#### 3.4. Beta diversity

Significant differences were identified in microbiome structure in gill ( $F_{5,81} = 46.592$ ,  $R_2 = 0.742$ ,  $p < 0.001$ ), skin ( $F_{5,71} = 25.991$ ,  $R_2 = 0.64669$ ,  $p < 0.001$ ) and hindgut ( $F_{5,72} = 3.7641$ ,  $R_2 = 0.20723$ ,  $p < 0.001$ ) over time. PERMANOVA also identified significant differences between tissues ( $F_{5,244} = 17.939$ ,  $R_2 = 0.1807$ ,  $p < 0.001$ ). Beta diversity was calculated using Bray-Curtis distances and values for gill, skin and hindgut at individual timepoints are plotted in an NMDS plot in Fig. 3. In gill and skin, significant differences in communities were identified between all timepoints (all at  $p < 0.001$ ). In hindgut, significant differences were identified between FW2 and all other timepoints ( $p < 0.05$ ) with the exception of FW3 and SW2. FW3 was distinct from FW4 and SW1 ( $p < 0.05$ ) while SW2 was distinct from FW1, FW4 and SW1 ( $p < 0.01$ ). It should be noted that only five hindgut samples were retained at FW2 post-rarefaction due to low read counts in comparison to other sampling points.

#### 3.5. Microbial community composition in hindgut, gill and skin

Microbial community composition at the phylum level was determined at each sampling point for hindgut, gill, skin, water and diet samples. 13 phyla were present at a relative abundance  $>1\%$  in at least one sampling point and one tissue (Fig. 4A). Seven phyla were present at  $>1\%$  in gill, nine in skin, nine in hindgut, eight in loch water and just four in diet. Phylum composition was visibly stable in FW loch water.

**Table 1**

Fork length, weight, condition factor and specific growth rate in Atlantic salmon smolts during parr-smolt transformation ( $n = 3$  cages, 18 fish, means  $\pm$  SD). CF: condition factor, SGR: specific growth rate, NKA: ATPase activity. Degree days are expressed relative to onset of the spring photoperiod (LL – constant light). Temperature is rearing water temperature. Significant changes between sampling points were determined by ANOVA and superscript letters denote pairwise significance (Tukey's HSD test).

	FW1 13th Aug	FW2 12th Sept	FW3 11th Oct	FW4 12th Dec	SW1 23rd Dec	SW2 16th Jan
Water	FW LOCH	FW LOCH	FW LOCH	FW LOCH	SW LOCH	SW LOCH
Temperature (°C)	16.8	12.5	10.6	5.7	7.9	8.1
Photoperiod	15h15L:8h45D	13h00L:11h00D	10h45L:13h15D	LL	6h30L:17h30D	7h30L:16h30D
Degree days (dd)	-904.00	-457.65	-111.65	364.02	-	-
Length (cm)	$14.8 \pm 0.4^a$	$17.1 \pm 0.6^b$	$19.7 \pm 0.3^b$	$23.9 \pm 0.3^{bc}$	$24.6 \pm 1.3^c$	$27.2 \pm 1.6^d$
Weight (g)	$44.8 \pm 3.4^a$	$65.4 \pm 6.5^a$	$101.5 \pm 5.4^{ab}$	$154.8 \pm 3.3^{bc}$	$163.0 \pm 26.4^c$	$230.2 \pm 45.7^d$
CF	$1.45 \pm 0.03^a$	$1.28 \pm 0.02^b$	$1.32 \pm 0.01^b$	$1.12 \pm 0.02^c$	$1.08 \pm 0.00^c$	$1.11 \pm 0.03^c$
SGR (%)	-	$1.2 \pm 0.2^a$	$1.5 \pm 0.2^a$	$0.7 \pm 0.6^a$	$0.4 \pm 1.3^a$	$1.4 \pm 0.7^a$
Smolt score	-	$2.0 \pm 0.1^a$	$2.2 \pm 0.5^a$	$3.3 \pm 0.2^b$	-	-
Plasma chloride (mM L <sup>-1</sup> )	-	$122.0 \pm 0.46^a$	$120.0 \pm 1.8^a$	$121.2 \pm 3.3^a$	$150.1 \pm 3.8^b$	$142.4 \pm 1.8^c$
Gill NKA (M mg prot <sup>-1</sup> h <sup>-1</sup> )	-	$3.63 \pm 1.00^a$	$4.87 \pm 0.45^a$	$13.09 \pm 2.33^b$	-	-

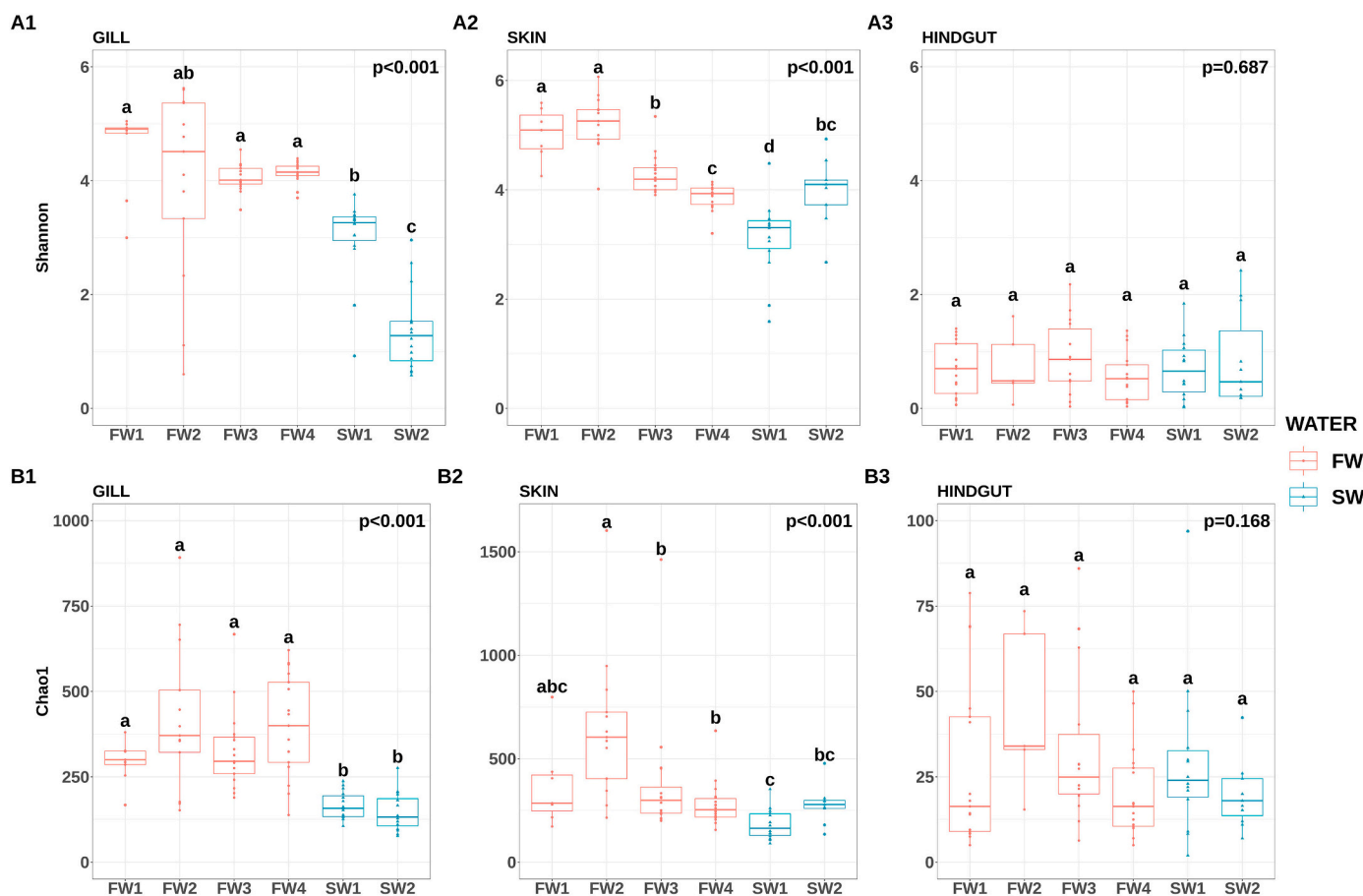


**Fig. 2.** Comparisons of alpha diversity [(A) Shannon] and richness [(B) Chao1]. (A1) Shannon: gill, (A2) Shannon: skin and (A3) Shannon: hindgut across sampling points. (B1) Chao1: gill, (B2) Chao1: skin and (B3) Chao1: hindgut. Red circles are individual samples in freshwater (FW) and blue triangles are individual samples in seawater (SW). Superscripts denote significant differences between sampling points determined by pairwise testing. (For interpretation of the references to colour in this figure legend, the reader is referred to the web version of this article.)

**Gill and skin.** The top 10 ASVs by relative abundance in each tissue are presented in Fig. 4B. Relative abundances of all ASVs are presented in Table S1. At FW1 and FW2 gill and skin communities were differentiated by the relative abundance of the phylum *Chlamydiae*. The top two taxa in gill at FW1 were ASV168 (*Candidatus Rubidus*) and ASV40 (*f. Chlamydiaceae*), constituting as much as 38.2–41.3% in some individuals. ASV40 dominance persisted at FW2 (up to 92.4%). BLASTn determined ASV40 to be *Candidatus Clavichlamydia salmonicola* (Accession LN995851.1; 100% identity and 99.77% cover). *Chlamydiae* sp. constituted <3% of total relative abundance in FW skin compared to 13.8% (FW1) and 31.9% (FW2) in gill. In contrast, there was remarkable similarity between gill and skin at FW3 and FW4. At FW3, the most abundant taxa in both tissues were a *Proteobacteria* of the genus *Novosphingobium* (ASV48) and three taxa belonging to the family *Burkholderiaceae*: *Cupriavidus* (ASV63), *Variovorax* (ASV95) and *Undibacterium* (ASV121). At FW4, two *Burkholderiaceae* of the genus *Janthinobacterium* (ASV13 and ASV32) were dominant. In SW, gill and skin microbial communities were again distinguished by the presence / absence of *Chlamydiae* sp. At SW1, taxa belonging to the phylum *Firmicutes* were the most abundant in skin (ASV45; *Brochothrix*) and (ASV41; *Weissella*) and a *Proteobacteria* of the family *T34* (ASV55) was prominent in a small number of individuals. Gill also harboured ASV45 and ASV41, but was dominated by ASV10, a *Chlamydiae* sp. ASV10 was also present at FW2, but at only 1.3% total relative abundance across all individuals. At sampling point SW2, ASV10 completely dominated the community in gill, constituting 71.2% of total relative abundance and as much as 91.7% in individuals. As for the FW2 dominant ASV40, BLASTn determined ASV10 to be a distinct *Ca. C. salmonicola* (Accession

LN995846.1; 100% identity and cover).

**Hindgut.** In the hindgut, there was a high level of interindividual variability with a single or very few ASVs constituting almost 100% relative abundance in individual communities in many cases. Dominant taxa in the hindgut were distinct from those identified in gill and skin. At FW1 ASV1 (genus *Brevinema*) constituted 41.2% of the total relative abundance across all individuals, increasing to 62.4% at FW4. Dominance of ASV1 continued to SW1 (53.5%) but was replaced by ASV5 (genus *Mycoplasma* – 47.5%) at SW2. ASV1 and ASV5 were not present in the microbiota of any of the diet samples analysed, as was also the case for ASV17 (*f. Ruminococcaceae*), ASV8 (*GCA-900066225*) ASV39 (*Romboutsia*) and ASV42 and ASV61 (*f. Desulfovibrionaceae*) while ASV17 (*f. Ruminococcaceae*) was present at just 0.07% in FW4 diet only.

### 3.6. 'Core' microbiota

Core taxa were defined as those present in 90% samples at 0.1% or more relative abundance (Table S2). No cores were identified across all sampling points in any mucosal surface. Considering FW alone for external tissues, four cores were identified in skin - two belonging to the *Actinobacteria* family *Sporichthyaceae* (ASV84 and ASV112) and two to the *Proteobacteria Burkholderiaceae* family (ASV94 and ASV159). These same four cores were identified in gill alongside an additional ASV belong to *Sporichthyaceae* (ASV107). There were two cores in gill in SW, both belonging to *Chlamydiaceae* (ASV10 and ASV40) while a single taxa of the genus *Plactomicrobium* was identified as a SW core in skin (ASV325). At individual sampling points in gill the numbers of core taxa identified were 25, 14, 40, 54, 13 and 5, while in skin 11, 22, 35, 60, 11

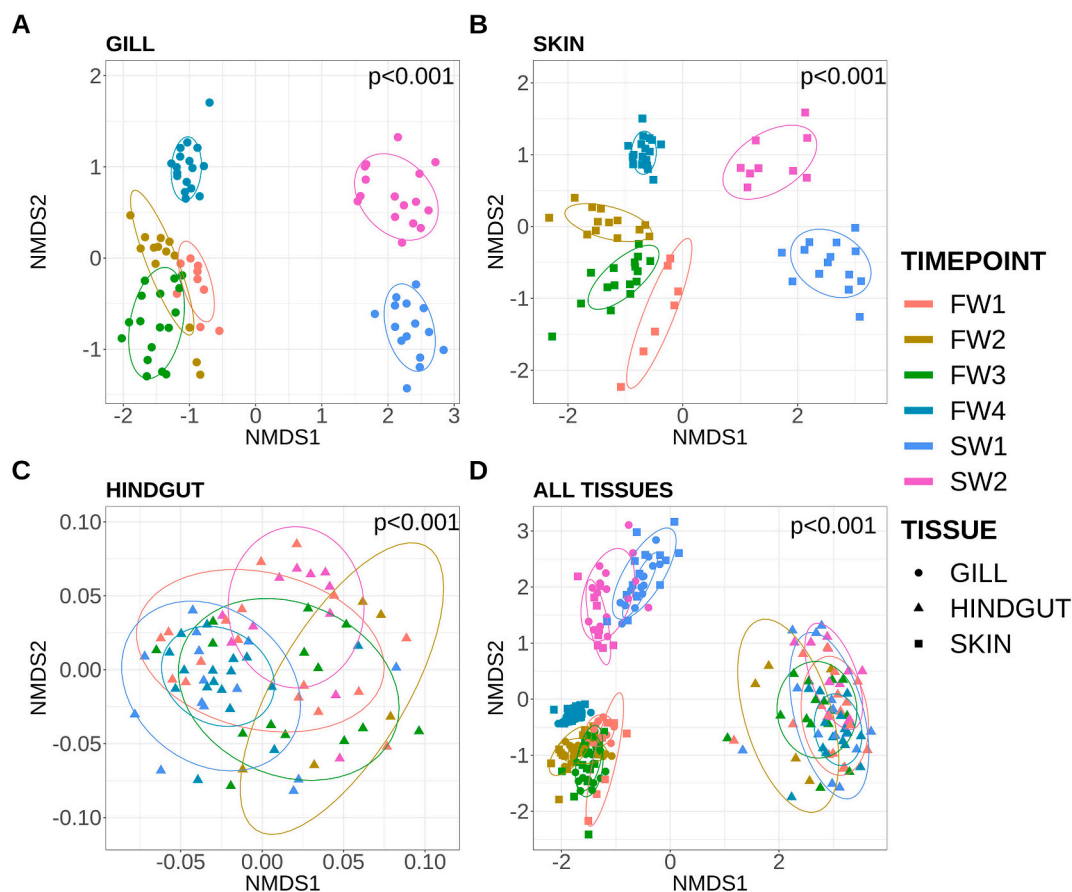


**Fig. 3.** Bray-Curtis distances visualized in NMDS plots. Sampling points are distinguished by colour while different marker shapes indicate source (gill, skin, hindgut or water). Beta diversity within gill samples is presented in (A) skin in (B) and hindgut in (C). (D) depicts beta diversity in different sample types, including three mucosal tissues and water. Visual summaries are provided with data ellipses based upon an assumed multivariate t-distribution are drawn at a level of 0.75.

and 7 cores were identified. In the hindgut a single ASV (ASV1) belonging to the genus *Brevinema* was identified as core at FW1 and FW4 and one *Mycoplasma* (ASV5) at SW2. Reducing stringency to 80% of samples at 0.1% or more relative abundance, both ASV1 and ASV5 were considered core hindgut taxa across the entire study.

Considering external cores only it was evident that there were extensive blocks of core taxa specific to FW3, FW4 and SW1 in particular (Fig. S2). There was a high degree of overlap of core taxa between gill and skin at all timepoints with the notable exceptions of ASV10 and ASV40, *Chlamydiae* sp. which were specific to gill. ASV10 and ASV40 were not identified in corresponding SW water samples and ASV40 was present only in FW3 at a low relative abundance of just 0.02%. Additionally, the majority of single sampling point core in FW were not identified in the corresponding water sample (with the exception of those specific to FW1), but the majority of those present in gill and skin throughout FW sampling (particularly ASV84, ASV94, ASV107, ASV112, ASV159) were also identified in FW water samples throughout (Fig. 5). These five core taxa were also identified in SW water samples although in SW they were no longer identified as cores.

#### 4. Discussion

Mucosal surfaces and their associated microbiota play an important role in host defences against infection by bacterial pathogens. We characterized temporal dynamics of microbiome composition in Atlantic salmon gill, skin and hindgut and identified distinct patterns in each tissue. In skin and gill a decline in diversity was identified over time in FW, indicative of maturation of the microbiome while hindgut diversity remained stable. Post-SWT gill and skin microbial communities declined

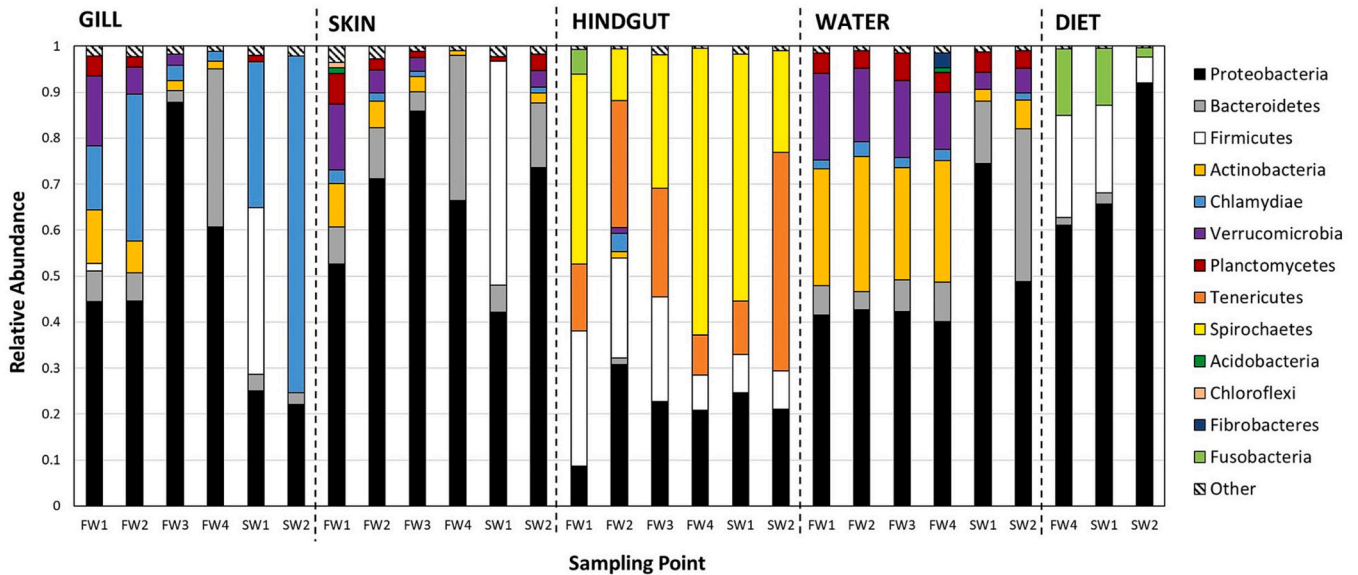
further in diversity but the skin microbiome re-established to pre-transfer levels of diversity and richness after one month in SW while the gill community became increasingly dominated by a single ASV identified as the *Chlamydiae* species *Candidatus Clavichlamydia salmonicola*. This study highlights tissue specific dynamics in mucosal microbiota and the potential for proliferation of opportunistic bacteria at a pivotal, but vulnerable life history stage in a commercially important species. To our knowledge the only other studies of longitudinal microbiome composition in multiple tissues under ambient conditions have been performed in seawater with Pacific chub Mackerel (*Scomber japonicus*) (Minich et al., 2020b) and European seabass (*Dicentrarchus labrax*) (Rosado et al., 2021a).

##### 4.1. Time a stronger driver of microbiome composition than mucosal surface

Despite differences in temporal dynamics and community composition between mucosal surfaces, analysis of beta-diversity at the ASV level revealed greater separation between sampling points than between the two external mucosal surfaces at individual sampling points. Body site has previously been identified as the strongest driver of microbial composition in single timepoint studies (Lowrey et al., 2015; Minich et al., 2020a; Bledsoe et al., 2022). However, a key factor in the current study is the natural decline in water temperature throughout the study (range 16.8 to 5.7 °C). Bacteria are highly sensitive to temperature (Corkrey et al., 2012) and water temperature plays an influential role in determining commensal microbiomes (Minich et al., 2020b; Rosado et al., 2021a).

In European seabass sampled every month during farming in a semi-

A



B

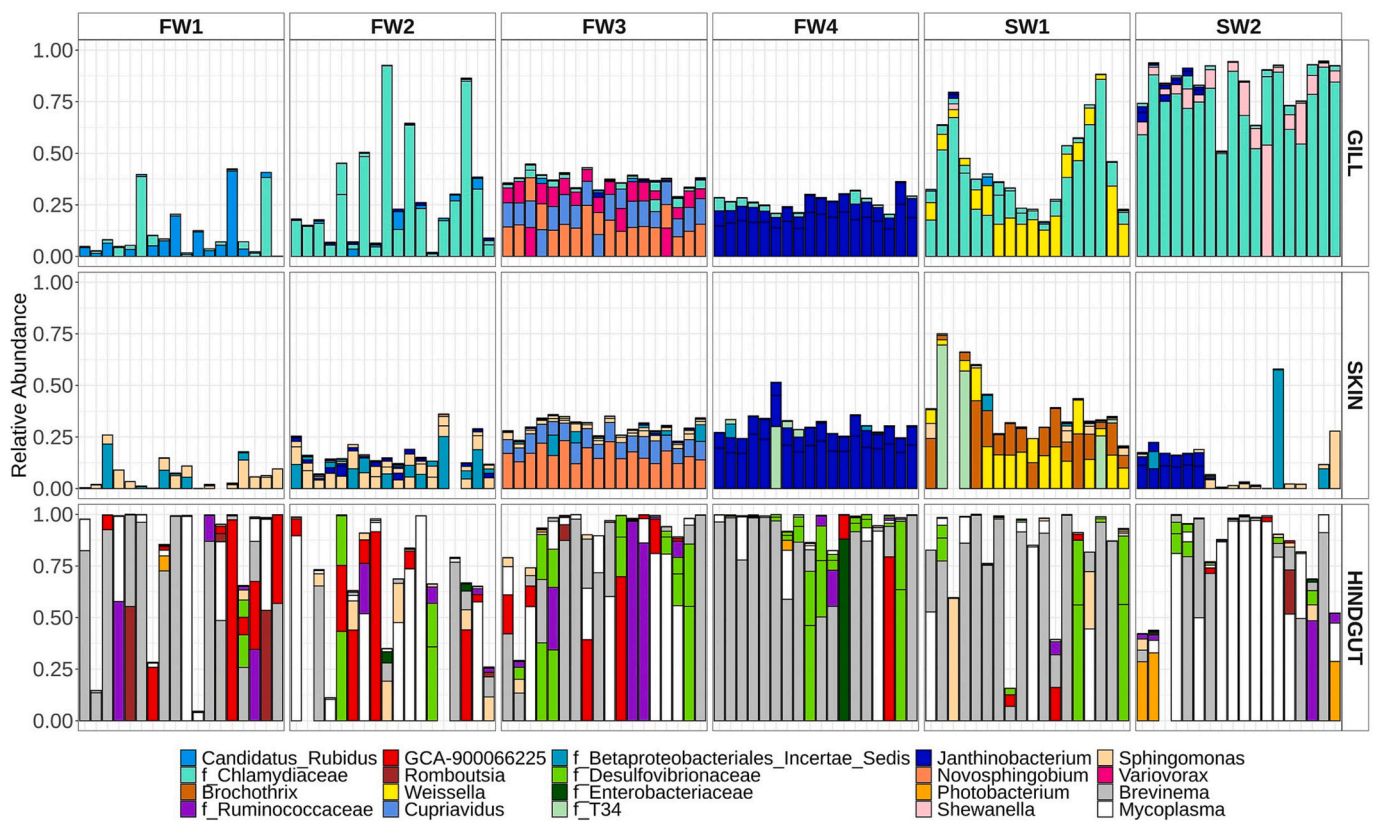


Fig. 4. (A) Microbial community composition in gill, skin, hindgut, water and diet at the phylum level. y-axis represents relative abundance of each phylum and x-axis individual sampling points. Phyla are represented in columns as different colours. (B) Community composition at the genus level of the top 10 taxa in each tissue sampled.

intensive pond, distinct communities were identified throughout the year over a temperature range of 13.3 to 25.1 °C and analysis of skin and gill microbiome communities indicated a complex exchange of microbes inhabiting the two external mucosal sites over time (Rosado et al., 2021b). Yet in a longitudinal study of Pacific chub mackerel with varying natural temperature, body site was still determined as the main

driver of microbiome composition although environmental parameters including temperature and chlorophyll-a concentration, and biological parameters including fish age had broad effects on microbial composition in gill and skin (Minich et al., 2020b). In a RAS with fish of the same genetic stock used in the present study (Lorgen-Ritchie et al., 2022) again there was greater separation between sampling points than

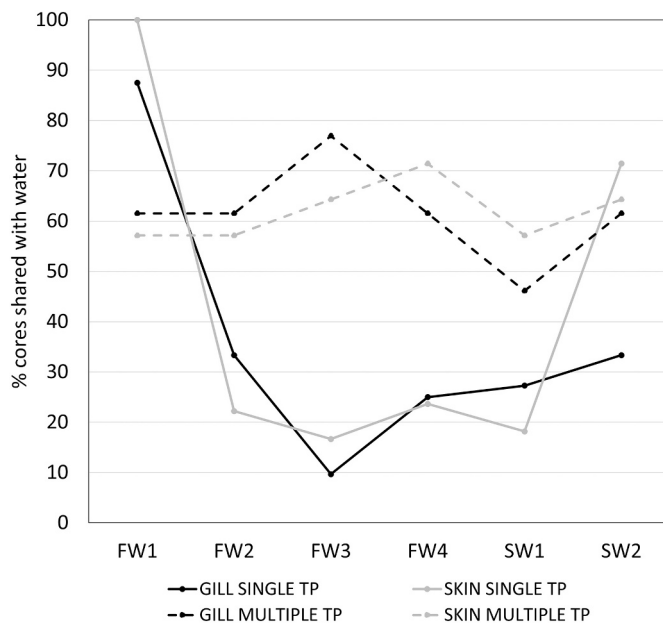


Fig. 5. The percentage of core taxa identified in gill and skin at single or multiple time points (TP) also identified in water samples at each sampling point.

between skin and gill at individual time points despite a narrow temperature range from 14.3 to 17.2 °C. It is likely that temperature interacts with additional environmental and host parameters to determine temporal patterns.

The internal hindgut microbiome was distinct from external skin and gill microbiomes throughout the study. Diversity and richness were stable throughout the study along with characteristic inter-individual variability. Individual taxa from the genera *Brevinema* or *Mycoplasmata* often dominated entire communities in individuals. Both taxa have been identified as prevalent in the gut in numerous studies in salmon at various life stages in both FW and SW with community compositions often dominated by few taxa (Llewellyn et al., 2016; Dehler et al., 2017; Uren Webster et al., 2018; Gupta et al., 2019; Uren Webster et al., 2020; Li et al., 2021). In a temporal study following smolts at 4-weeks, 6 months and 11 months post-SWT, *Mycoplasmata* prevalence increased only after 6 months in SW, although composition was dominated by lactic acid bacteria (LAB). Additionally, *Photobacterium* dominated at 4 weeks post-SWT, with only a few individuals displaying high prevalence of *Brevinema* (Wang et al., 2021). A comparative study identified higher prevalence of *Brevinema* in mucosa compared to digesta (Li et al., 2021) but another identified *Brevinema* as a core in both mucosa and digesta (Gupta et al., 2019). Mucosa and digesta were sequenced together in the current study therefore no distinction can be made. A recent translocation experiment suggested a role of early rearing environment in determining *Brevinema* prevalence in later life stages (Uren Webster et al., 2020). Similarly, non-neutral selection on *Mycoplasmata* indicate that these taxa are selectively retained by the host following early life exposure (Heys et al., 2020) and presence of *Mycoplasmata* has been proposed as a biomarker of Atlantic salmon health (Bozzi et al., 2021). However, other studies have identified low or no relative abundance of *Mycoplasmata* in Atlantic salmon reared in both RAS and flow-through systems (Minich et al., 2020a; Lorgen-Ritchie et al., 2021) and in seawater cages (Zarkasi et al., 2016). Diet can be a strong driver of microbial colonization in the gut, yet in this study the dominant microbial taxa in the hindgut were absent in the organic diet and a change in pellet size had no apparent impact on hindgut microbiome diversity, richness or composition.

#### 4.2. Distinct microbiome dynamics in gill, skin and hindgut during FW rearing and post-SWT

Similar to previous studies including multiple mucosal surfaces, alpha diversity was higher in external surfaces when compared to hindgut throughout the study (Uren Webster et al., 2018). The decline in diversity in skin throughout FW rearing is indicative of stabilization and specialization of the microbial community, with a heightened role for host-specific regulation, interaction between microbes and active dispersal (Burns et al., 2016; Stephens et al., 2016). Higher evenness in FW compared to SW in skin mucus (Lokesh and Kiron, 2016) was determined to be indicative of the formation of a stable bacterial community in FW, a feature of functional stability and resilience (Wittebolle et al., 2009) followed by disruption upon entry to seawater. Maturation of communities coincided with declining water temperature, but also with fish age, both of which are known to impact microbiome composition (Lokesh et al., 2019; Minich et al., 2020b). Additionally, routine disinfection treatments were applied during FW rearing which have the potential to impact microbial diversity (Bozzi et al., 2021). Rearing environment can also impact microbial richness and similarities between mucosal body sites (Minich et al., 2020a). The dynamics during open loch FW culture were in contrast to those in a cohort of fish of the same genetic background reared in a FW recirculating aquaculture system (RAS) where there were rising trends in diversity and richness over time in FW, attributed to increased organic load in the system (Lorgen-Ritchie et al., 2021; Lorgen-Ritchie et al., 2022). The routine disinfection treatments applied in FW lochs are not utilised to the same extent in RAS which could partially account for the differences in temporal dynamics. In addition, fish in the present study were fed organic diets which are higher in fishmeal and fish oil content than regular diet formulations. Differences in stability in gill, skin and hindgut communities throughout rearing in the FW loch in terms of diversity and richness indicate different selective pressures at work in each mucosal niche.

SWT is a key transitional period in the life history of Atlantic salmon that is accompanied by increased susceptibility to infectious disease (Aunsmo et al., 2008) and health challenges to tissues such as gill (Król et al., 2020), a potential consequence of systemic suppression of immunity during PST (Johansson et al., 2016). In FW loch-reared smolts, diversity and richness in both gill and skin mucus declined significantly one week following transfer to seawater, accompanied by a distinct shift in community composition with an increased presence of the phylum *Firmicutes*. Salinity acts as a barrier to microbes (Logares et al., 2009; Logares et al., 2013) and SWT is accompanied by distinct shifts in microbiome composition in gill (Lorgen-Ritchie et al., 2022), skin (Lokesh and Kiron, 2016) and gut (Dehler et al., 2017). In the present study, there was no distinct change in community composition in the hindgut following transfer from a FW to SW loch. This could be a consequence of fish being exposed to a greater variety of microbes in the FW rearing phase compared to those reared in more sterile RAS or flow-through systems. Additionally, Atlantic salmon reared in land-based facilities tend to be reared at optimum temperatures for growth (~12–16 °C) and can experience a temperature shift despite acclimation protocols (up or down depending on smolt cohorts and time of transfer) in conjunction with salinity change during SWT in temperate climates with year-round production. In contrast, the fish in this study were exposed to a natural temperature decline prior to transfer to a SW site at similar temperature (+2 °C).

Results showed skin microbial community re-established itself with diversity, richness and phylum composition comparable to pre-transfer (FW4), but with an entirely different community composition at the ASV level. This contrasted with gill microbial diversity which continued to decline as a result of a single dominant potentially pathogenic ASV belonging to the genus *Chlamydiae*. In fish with the same genetic background reared in FW RAS, diversity remained constant in external mucosal sites following SWT although entirely distinct communities



were established at the ASV level (Lorgen-Ritchie et al., 2022). Conversely, an increase in both metrics post-transfer was determined in skin in a non-commercial flow-through system at a constant temperature of 12 °C (Lokesh and Kiron, 2016). It must be acknowledged that fish in the present study were transferred to SW in winter while those from the RAS study were transferred in summer, and studies have shown seasonality to be a factor in determining microbial composition (Zarkasi et al., 2014). Temperature can also impact biological processes including both specific and non-specific immunity (Abram et al., 2017). Furthermore, feed intake can be reduced post-SWT, with as few as 10% of individuals feeding normally in the first week post-transfer (Stradmeier, 1994) and food deprivation can cause a rapid decrease in the number of epidermal mucus cells of the lateral skin, potentially decreasing mucus secretion and explaining some differences in the diversity of mucus-dwelling microbiota (Landeira-Dabarca et al., 2013).

#### 4.3. Persistent taxa in gill and skin mucosa also identified in rearing water

In support of the formation of stable functional communities in external mucosa over time in FW, the number of taxa identified as core in both skin and gill mucus increased over time in FW, indicative of reduced inter-individual variability. The identity of core taxa was time point specific at the ASV level although many belonged to the *Proteobacteria* family *Burkholderiaceae*. *Proteobacteria* also constituted the majority of 11 identified cores in skin across an array of natural and captive populations of Atlantic salmon (Uren Webster et al., 2018). Succession of core taxa was apparent, dominated by the *Verrucomicrobia* phylum at FW1 and *Proteobacteria* and *Bacteroidetes* at FW2-FW4. Such succession could be a consequence of change in environmental parameters such as temperature (Rosado et al., 2021a). For example, temperature declined from 10.3 to 5.7 °C between FW3 and FW4. Routine disinfection could also play a role. Core taxa numbers declined post-SWT and were predominantly of the phylum *Firmicutes* at SW1.

It was in the past hypothesized that external teleost microbiome compositions are simply a consequence of colonization by strains in the environment (Horsley, 1973), but this assumption has been repeatedly challenged for adult fish (Legrand et al., 2018; Rosado et al., 2021a). During early development, environmental conditions will play an important role in determining the composition of the initial colonising community (Minich et al., 2021). However, the mucosal immune system allows the host to 'select' for symbionts to some degree, enabling maintenance of community homeostasis, for example via immunoglobulin (Ig) coating of microbes which aids in selectivity (Woof and Mestecky, 2005; Kelly and Salinas, 2017). In the present study, the small number of core ASVs present throughout the study period in both skin and gill mucus were also identified in water throughout, but the higher numbers of cores specific to individual time points were most often absent from the corresponding water sample. Atlantic salmon and brook charr (*Salvelinus fontinalis*) skin mucus microbiomes tend to overlap water communities at the phylum or even genus level (Boutin et al., 2013; Minniti et al., 2017; Uren Webster et al., 2018), but in these same studies, beta-diversity analyses separates communities from the different niches despite the direct contact of skin with the environment, indicative of specific adaptation of certain taxa to the skin mucosa. As a further example of the distinct nature of mucosal communities, ASV10 (phylum *Chlamydiae*) was identified as a SW core in gill, completely dominating community composition by SW2, but this ASV was not identified in the surrounding water at any sampling point despite other members of the phylum *Chlamydiae* being present at low relative abundance.

#### 4.4. Dominance of *Chlamydia* sp. in gill mucosa post-SWT

Gill community composition could be distinguished from that of skin at FW2 by a transient increase in the relative abundance of a single taxon belonging to the phylum *Chlamydiae* in the majority of fish, which

BLASTn revealed as *Candidatus Clavichlamydia salmonicola*. Post-SWT transfer a second taxon predicted by BLASTn was *Ca. C. salmonicola* which increased in many fish after 1-week and dominated in all by 4-weeks post-SWT. The taxon identified at FW2 was also identified as a SW core, but at far lower relative abundance. Despite high prevalence in SW, a natural FW origin of *Ca. C. salmonicola* has been hypothesized (Schmidt-Posthaus et al., 2012) and indeed in the current study, taxa belonging to the *Chlamydiae* phylum were identified during FW sampling, albeit at very low levels. Members of the phylum *Chlamydia* have been identified as causative agents in epitheliocystis cytoplasmic membrane-bound inclusions containing gram-negative bacteria in gill, and less commonly, skin epithelium and have been implicated in proliferative gill inflammation (PGI) (Karlsen et al., 2008).

The absence of clinical disease in the presence of epitheliocysts is possible and the presence of bacterial agents including *Candidatus piscichlamydia salmonis* (Steinum et al., 2009) and *Ca. C. salmonicola* (Mitchell et al., 2010) have been sequenced in apparently healthy fish. *Ca. C. salmonicola* was shown to disappear from the gills 4–6 weeks post-SWT (Mitchell et al., 2010). Similar scenarios exist in human skin microbiomes, for example *Propionibacterium acnes* is a producer of metabolites that deter infection by pathogens, but certain strains of the same species appear to have a causative role in acne (Fitz-Gibbon et al., 2013). A betaproteobacterium, *Candidatus branchiomonas*, present in SW gills in this study at 1–2% relative abundance, has also been identified in cysts, and was the dominant taxa in the gills of both resistant and susceptible lines of rainbow trout, identified at very high relative abundance in healthy fish (Toenshoff et al., 2012; Brown et al., 2019; Brown et al., 2021).

## 5. Conclusions

Mucosal microbiomes are important components of host resistance to disease and growth performance in aquaculture, but little is known about how their composition changes with time. In this study we analysed the temporal dynamics of microbial communities in the gill, skin and hindgut of Atlantic salmon reared in an open FW loch and following SWT. Temporal declines in diversity in FW were accompanied by an increase in the number of core taxa, suggestive of functional stabilization of external microbial community over time in FW. The impact of rearing time needs to be considered in parallel with environmental factors such as seasonal water temperature declines, salinity change, feed formulations and routine disinfection practices as these parameters change concurrently with rearing time. These results build on previous longitudinal studies in RAS to contribute to an understanding of the key drivers of microbiome dynamics in different FW rearing systems and subsequent consequences for smolt robustness following transfer to sea.

Supplementary data to this article can be found online at <https://doi.org/10.1016/j.aquaculture.2022.739211>.

### Ethics approval and consent to participate

Ethical review and approval was not required for the animal study because the sampling of fish was carried out under established protocols for routine health assessments in accordance with RSPCA Assured Welfare Standards for farmed Atlantic salmon.

### Availability of data and materials

The datasets presented in this study can be found in online repositories. The names of the repository/repositories and accession number(s) can be found below: <https://www.ncbi.nlm.nih.gov/bioproject/PRJNA853150>.

### Funding

This work was supported by the UKRI project ROBUSTSMOLT [grant

numbers BBSRC BB/S004270/1 and BB/S004432/1]. There was also co-funding from the Scottish Aquaculture Innovation Centre.

### Author statement

SM, JT, and HM designed the experiment. MC, JT, and LC were responsible for management of fish parameters and smolt indicator analyses. ML-R, LC, and MC conducted the sample collection. ML-R performed the DNA extraction and preparation of samples for 16S sequencing and downstream bioinformatic data analyses, and wrote the initial manuscript draft which was reviewed and edited by SM, HM, and JT. All authors contributed to the article and approved the submitted version.

### Declaration of Competing Interest

The authors declare that they have no known competing financial interests or personal relationships that could have appeared to influence the work reported in this paper.

### Data availability

The datasets presented in this study can be found at <https://www.ncbi.nlm.nih.gov/bioproject/PRJNA853150>.

### Acknowledgements

The authors would like to thank John Richmond and staff at MOWI and the Centre for Genome Enabled Biology and Medicine (CGEBM) at the University of Aberdeen, particularly Dr. Ewan Campbell, for help with amplification protocols, conducting 16S library preparation and sequencing.

### References

- Abram, Q.H., Dixon, B., Katzenback, B.A., 2017. Impacts of low temperature on the teleost immune system. *Biology* 6 (4), 39.
- Aunsmo, A., Bruheim, T., Sandberg, M., Skjerve, E., Romstad, S., Larssen, R.B., 2008. Methods for investigating patterns of mortality and quantifying cause-specific mortality in sea-farmed Atlantic Salmon *Salmo Salar*. *Dis. Aquat. Org.* 81 (2), 99–107.
- Bledsoe, J.W., Pietrak, M.R., Burr, G.S., Peterson, B.C., Small, B.C., 2022. Functional feeds marginally alter immune expression and microbiota of Atlantic Salmon (*Salmo Salar*) gut, gill, and skin mucosa though evidence of tissue-specific signatures and host-microbe coadaptation remain. *Anim. Microbiome* 4 (1), 20.
- Boutin, S., Bernatchez, L., Audet, C., Derôme, N., 2013. Network analysis highlights complex interactions between pathogen, host and commensal microbiota. *PLoS One* 8 (12) (Article e84772).
- Bozzi, D., Rasmussen, J.A., Carøe, C., Sveier, H., Nordøy, K., Gilbert, M.T.P., Limborg, M. T., 2021. Salmon gut microbiota correlates with disease infection status: potential for monitoring health in farmed animals. *Anim. Microbiome* 3 (1), 30.
- Bray, J.R., Curtis, J.T., 1957. An ordination of the upland Forest communities of southern Wisconsin. *Ecol. Monogr.* 27 (4), 326–349.
- Brown, R.M., Wiens, G.M., Salinas, I., 2019. Analysis of the gut and gill microbiome of resistant and susceptible lines of rainbow trout (*Oncorhynchus mykiss*). *Fish Shellfish Immunol.* 86, 497–506.
- Brown, R., Moore, L., Mani, A., Patel, S., Salinas, I., 2021. Effects of ploidy and salmonid alphavirus infection on the skin and gill microbiome of Atlantic Salmon (*Salmo Salar*). *PLoS One* 16 (2) (Article e0243684).
- Burns, A.R., Stephens, W.Z., Stagaman, K., Wong, S., Rawls, J.F., Guillemin, K., Bohannan, B.J.M., 2016. Contribution of neutral processes to the assembly of gut microbial communities in the zebrafish over host development. *The ISME Journal* 10 (3), 655–664.
- Callahan, B.J., McMurdie, P.J., Rosen, M.J., Han, A.W., Johnson, A.J.A., Holmes, S.P., 2016. DADA2: high-resolution sample inference from Illumina amplicon data. *Nat. Methods* 13 (7), 581–583.
- Chao, A., 1984. Nonparametric estimation of the number of classes in a population. *Scand. J. Stat.* 11 (4), 265–270.
- Clinton, M., Wyness, A.J., Martin, S.A.M., Brierley, A.S., Ferrier, D.E.K., 2021. Sampling the fish gill microbiome: a comparison of tissue biopsies and swabs. *BMC Microbiol.* 21 (1), 313.
- Corkrey, R., Olley, J., Ratkowsky, D., McMeekin, T., Ross, T., 2012. Universality of thermodynamic constants governing biological growth rates. *PLoS One* 7 (2) (Article e32003).
- Dehler, C.E., Secombes, C.J., Martin, S.A.M., 2017. Seawater transfer alters the intestinal microbiota profiles of Atlantic Salmon (*Salmo Salar* L.). *Sci. Rep.* 7 (1) (Article 13877).
- FAO, 2020. The State of World Fisheries and Aquaculture: Sustainability in Action. Food and Agriculture Organization of the United Nations, Rome.
- FAO, 2022. The State of World Fisheries and Aquaculture: Towards Blue Transformation. Food and Agriculture Organization of the United Nations, Rome.
- Fitz-Gibbon, S., Tomida, S., Chiu, B.-H., Nguyen, L., Du, C., Liu, M., Elashoff, D., et al., 2013. *Propionibacterium acnes* strain populations in the human skin microbiome associated with acne. *J. Invest. Dermatol.* 133 (9), 2152–2160.
- Glover, C.N., Bucking, C., Wood, C.M., 2013. The skin of fish as a transport epithelium: a review. *J. Comp. Physiol. B.* 183 (7), 877–891.
- Gomez, D., Sunyer, J.O., Salinas, I., 2013. The mucosal immune system of fish: the evolution of tolerating commensals while fighting pathogens. *Fish Shellfish Immunol.* 35 (6), 1729–1739.
- Gupta, S., Fečkaninová, A., Lokesh, J., Koščová, J., Sørensen, M., Fernandes, J., Kiron, V., 2019. *Lactobacillus* dominate in the intestine of Atlantic Salmon fed dietary probiotics. *Front. Microbiol.* 9, 3247.
- Heys, C., Cheab, B., Busetti, A., Kazlauskaitė, R., Maier, L., Sloan, W.T., Ijaz, U.Z., Kaufmann, J., McGinnity, P., Llewellyn, M.S., 2020. Neutral processes dominate microbial community assembly in Atlantic Salmon, *Salmo Salar*. *Appl. Environ. Microbiol.* 86 (8) (Article e02283-19).
- Horsley, R.W., 1973. The bacterial Flora of the Atlantic Salmon (*Salmo Salar* L.) in relation to its environment. *J. Appl. Bacteriol.* 36 (3), 377–386.
- Johansson, L.-H., Timmerhaus, G., Afanasyev, S., Jørgensen, M., Krasnov, A., 2016. Smoltification and seawater transfer of Atlantic Salmon (*Salmo Salar* L.) is associated with systemic repression of the immune transcriptome. *Fish Shellfish Immunol.* 58, 33–41.
- Karlsen, M., Nylund, A., Watanabe, K., Helvik, J.V., Nylund, S., Plarre, H., 2008. Characterization of ‘*Candidatus Clavochlamydia Salmonicola*’: an intracellular bacterium infecting salmonid fish. *Environmen. Microbiol.* 10 (1), 208–218.
- Kelly, C., Salinas, I., 2017. Under pressure: interactions between commensal microbiota and the teleost immune system. *Front. Immunol.* 8, 559.
- Khaw, H.L., Gjerde, B., Boison, S.A., Hjelle, E., Difford, G.F., 2021. Quantitative genetics of Smoltification status at the time of seawater transfer in Atlantic Salmon (*Salmo Salar*). *Front. Genet.* 12 (Article 696893).
- Klindworth, A., Pruesse, E., Schweer, T., Peplies, J., Quast, C., Horn, M., Glöckner, F.O., 2013. Evaluation of general 16S ribosomal RNA gene PCR primers for classical and next-generation sequencing-based diversity studies. *Nucleic Acids Res.* 41 (1) (Article e1).
- Kolarevic, J., Baeverfjord, G., Takle, H., Ytteborg, E., Reiten, B.K.M., Nergård, S., Terjesen, B.F., 2014. Performance and welfare of Atlantic Salmon Smolt reared in recirculating or flow through aquaculture systems. *Aquaculture* 432, 15–25.
- Kolde, R., 2012. Pheatmap: Pretty Heatmaps. R Package Version 1.0.12. <https://CRAN.R-project.org/package=pheatmap>.
- Król, E., Noguera, P., Shaw, S., Costelloe, E., Gajardo, K., Valdenegro, V., Bickerdike, R., Douglas, A., Martin, S.A.M., 2020. Integration of transcriptome, gross morphology and histopathology in the gill of sea farmed Atlantic Salmon (*Salmo Salar*): lessons from multi-site sampling. *Front. Genet.* 11, 610.
- Lahti, L., Shetty, S.A., 2017. Tools for Microbiome Analysis in R. R Package Version 1.7.21. <http://microbiome.github.com/microbiome>.
- Landeira-Dabarca, A., Steiro, C., Álvarez, M., 2013. Change in food ingestion induces rapid shifts in the diversity of microbiota associated with cutaneous mucus of Atlantic Salmon *Salmo Salar*. *J. Fish Biol.* 82 (3), 893–906.
- Legrand, T.P.R.A., Catalano, S.R., Wos-Oxley, M.L., Stephens, F., Landos, M., Bansemer, M.S., Stone, D.A.J., Qin, J.G., Oxley, A.P.A., 2018. The inner workings of the outer surface: skin and gill microbiota as indicators of changing gut health in yellowtail kingfish. *Front. Microbiol.* 8, 2664.
- Li, Y., Bruni, L., Jaramillo-Torres, A., Gajardo, K., Kortner, T.M., Krogdahl, Å., 2021. Differential response of Digesta- and mucosa-associated intestinal microbiota to dietary insect meal during the seawater phase of Atlantic Salmon. *Anim. Microbiome* 3 (1), 8.
- Llewellyn, M.S., McGinnity, P., Dionne, M., Letourneau, J., Thonier, F., Carvalho, G.R., Creer, S., Derome, N., 2016. The biogeography of the Atlantic Salmon (*Salmo Salar*) gut microbiome. *ISME J.* 10 (5), 1280–1284.
- Logares, R., Bråte, J., Bertilsson, S., Clasen, J.L., Shalchian-Tabrizi, K., Rengefors, K., 2009. Infrequent marine–freshwater transitions in the microbial world. *Trends Microbiol.* 17 (9), 414–422.
- Logares, R., Lindström, E., Langenheder, S., Logue, J.B., Paterson, H., Laybourn-Parry, J., Rengefors, K., Tranvik, L., Bertilsson, S., 2013. Biogeography of bacterial communities exposed to progressive long-term environmental change. *ISME J.* 7 (5), 937–948.
- Lokesh, J., Kiron, V., 2016. Transition from freshwater to seawater reshapes the skin-associated microbiota of Atlantic Salmon. *Sci. Rep.* 6 (1) (Article 19707).
- Lokesh, J., Kiron, V., Sipkema, D., Fernandes, J.M.O., Moum, T., 2019. Succession of embryonic and the intestinal bacterial communities of Atlantic Salmon (*Salmo Salar*) reveals stage-specific microbial signatures. *MicrobiologyOpen* 8 (4) (Article e00672).
- Lorgen-Ritchie, M., Clarkson, M., Chalmers, L., Taylor, J.F., Migaud, H., Martin, S.A.M., 2021. A temporally dynamic gut microbiome in Atlantic Salmon during freshwater recirculating aquaculture system (RAS) production and post-seawater transfer. *Front. Mar. Sci.* 8, 869.
- Lorgen-Ritchie, M., Clarkson, M., Chalmers, L., Taylor, J.F., Migaud, H., Martin, S.A.M., 2022. Temporal changes in skin and gill microbiomes of Atlantic Salmon in a recirculating aquaculture system – why do they matter? *Aquaculture* 558 (Article 738352).

- Lowrey, L., Woodhams, D.C., Tacchi, L., Salinas, I., 2015. Topographical mapping of the rainbow trout (*Oncorhynchus Mykiss*) microbiome reveals a diverse bacterial community with antifungal properties in the skin. *Appl. Environ. Microbiol.* 81 (19), 6915.
- McCormick, S.D., 1993. Methods for nonlethal gill biopsy and measurement of Na<sup>+</sup>, K<sup>+</sup>-ATPase activity. *Can. J. Fish. Aquat. Sci.* 50 (3), 656–658.
- McCormick, S.D., 2012. Smolt physiology and endocrinology. In: McCormick, S.D., Brauner, C.J., Farrell, A.P. (Eds.), *Fish Physiology*, vol. 32. Academic Press, Amsterdam.
- McMurdie, P.J., Holmes, S., 2013. PhyloSeq: an R package for reproducible interactive analysis and graphics of microbiome census data. *PLoS One* 8 (4) (Article e61217).
- Minich, J.J., Poore, G.D., Jantawongsri, K., Johnston, C., Bowie, K., Bowman, J., Knight, R., Nowak, B., Allen, E.E., 2020a. Microbial ecology of Atlantic Salmon (*Salmo Salar*) hatcheries: impacts of the built environment on fish mucosal microbiota. *Appl. Environ. Microbiol.* 86 (12) (Article e00411-20).
- Minich, J.J., Petrus, S., Michael, J.D., Michael, T.P., Knight, R., Allen, E.E., 2020b. Temporal, environmental, and biological drivers of the mucosal microbiome in a wild marine fish, *Scomber Japonicus*. *mSphere* 5 (3) (Article e00401-20).
- Minich, J.J., Nowak, B., Elizur, A., Knight, R., Fielder, S., Allen, E.E., 2021. Impacts of the marine hatchery built environment, water and feed on mucosal microbiome colonization across ontogeny in yellowtail kingfish, *Seriola Lalandi*. *Front. Mar. Sci.* 8, 516.
- Minniti, G., Hagen, L.H., Porcellato, D., Jørgensen, S.M., Pope, P.B., Vaaje-Kolstad, G., 2017. The skin-mucus microbial community of farmed Atlantic Salmon (*Salmo Salar*). *Front. Microbiol.* 8, 2043.
- Mitchell, S.O., Steinum, T., Rodger, H., Holland, C., Falk, K., Colquhoun, D.J., 2010. Epitheliocystis in Atlantic Salmon, *Salmo Salar* L., farmed in fresh water in Ireland is associated with 'Candidatus *Clavochlamydia Salmonicola*' infection. *J. Fish Dis.* 33 (8), 665–673.
- Oksanen, J., Blanchet, F.G., Friendly, M., Kindt, R., Legendre, P., McGlinn, D., Minchin, P.R., et al., 2017. *Vegan: Community Ecology Package*. R Package Version 2.4-3. <https://CRAN.R-project.org/package=vegan>.
- Quast, C., Pruesse, E., Yilmaz, P., Gerken, J., Schweer, T., Yarza, P., Peplies, J., Glöckner, F.O., 2013. The SILVA ribosomal RNA gene database project: improved data processing and web-based tools. *Nucleic Acids Res.* 41, D590–D596.
- Rosado, D., Xavier, R., Cable, J., Severino, R., Tarroso, P., Pérez-Losada, M., 2021a. Longitudinal sampling of external mucosae in farmed European seabass reveals the impact of water temperature on bacterial dynamics. *ISME Commun.* 1 (1), 28.
- Rosado, D., Pérez-Losada, M., Pereira, A., Severino, R., Xavier, R., 2021b. Effects of aging on the skin and gill microbiota of farmed seabass and seabream. *Anim. Microbiome* 3 (1), 10.
- Salazar, G., 2020. *EcolUtils: Utilities for Community Ecology Analysis*. R Package Version 0.1. <https://github.com/GuillemSalazar/EcolUtils>.
- Salinas, I., Fernández-Montero, Á., Ding, Y., Sunyer, J.O., 2021. Mucosal immunoglobulins of teleost fish: a decade of advances. *Dev. Comp. Immunol.* 121, 104079.
- Schmidt-Posthaus, H., Polkinghorne, A., Nufer, L., Schifferli, A., Zimmermann, D.R., Segner, H., Steiner, P., Vaughan, L., 2012. A natural freshwater origin for two chlamydial species, *Candidatus Piscichlamydia Salmonis* and *Candidatus Clavochlamydia Salmonicola*, causing mixed infections in wild Brown trout (*Salmo Trutta*). *Environ. Microbiol.* 14 (8), 2048–2057.
- Shannon, C.E., 1948. A mathematical theory of communication. *The Bell Syst. Tech. J.* 27 (3), 379–423.
- Sigholt, T., Staurnes, M., Jakobsen, H.J., Åsgård, T., 1995. Effects of continuous light and short-day photoperiod on smolting, seawater survival and growth in Atlantic Salmon (*Salmo Salar*). *Aquaculture* 130 (4), 373–388.
- Slinger, J., Adams, M.B., Stratford, C.N., Rigby, M., Wynne, J.W., 2021. The effect of antimicrobial treatment upon the gill Bacteriome of Atlantic Salmon (*Salmo Salar* L.) and progression of amoebic gill disease (AGD) *in vivo*. *Microorganisms* 9 (5), 987.
- Steinum, T., Sjøstad, K., Falk, K., Kvellestad, A., Colquhoun, D.J., 2009. An RT-PCR-DGGE survey of gill-associated bacteria in Norwegian seawater-reared Atlantic Salmon suffering proliferative gill inflammation. *Aquaculture* 293 (3), 172–179.
- Stephens, W.Z., Burns, A.R., Stagaman, K., Wong, S., Rawls, J.F., Guillemin, K., Bohannan, B.J.M., 2016. The composition of the zebrafish intestinal microbial community varies across development. *ISME J.* 10 (3), 644–654.
- Stradmeyer, L., 1994. Survival, growth and feeding of Atlantic Salmon, *Salmo Salar* L., Smolts after transfer to sea water in relation to the failed Smolt syndrome. *Aquaculture Res.* 25 (1), 103–112.
- Toenshoff, E.R., Kvellestad, A., Mitchell, S.O., Steinum, T., Falk, K., Colquhoun, D.J., Horn, M., 2012. A novel betaproteobacterial agent of gill Epitheliocystis in seawater farmed Atlantic Salmon (*Salmo Salar*). *PLoS One* 7 (3) (Article e32696).
- Uren Webster, T.M., Consuegra, S., Hitchings, M., Garcia de Leaniz, C., 2018. Interpopulation variation in the Atlantic Salmon microbiome reflects environmental and genetic diversity. *Appl. Environ. Microbiol.* 84 (16) (Article e00691-18).
- Uren Webster, T.M., Rodriguez-Barreto, D., Castaldo, G., Gough, P., Consuegra, S., Garcia de Leaniz, C., 2020. Environmental plasticity and colonisation history in the Atlantic Salmon microbiome: a translocation experiment. *Mol. Ecol.* 29 (5), 886–898.
- Wang, J., Jaramillo-Torres, A., Li, Y., Kortner, T.M., Gajardo, K., Brevik, Ø.J., Jakobsen, J.V., Krogdahl, Å., 2021. Microbiota in intestinal digesta of Atlantic salmon (*Salmo salar*), observed from late freshwater stage until one year in seawater, and effects of functional ingredients: a case study from a commercial sized research site in the Arctic region. *Anim. Microbiome* 3, 14.
- Wickham, H., 2016. *Ggplot2: Elegant Graphics for Data Analysis*. Springer, New York.
- Wittebolle, L., Marzorati, M., Clement, L., Balloi, A., Daffonchio, D., Heylen, K., De Vos, P., Verstraete, W., Boon, N., 2009. Initial community evenness favours functionality under selective stress. *Nature* 458 (7238), 623–626.
- Woof, J.M., Mestecky, J., 2005. Mucosal Immunoglobulins. *Immunol. Rev.* 206 (1), 64–82.
- Xu, Z., Parra, D., Gómez, D., Salinas, I., Zhang, Y.-A., von Gersdorff Jørgensen, L., Heinecke, R.D., Buchmann, K., LaPatra, S., Sunyer, J.O., 2013. Teleost skin, an ancient mucosal surface that elicits gut-like immune responses. *Proc. Natl. Acad. Sci. U. S. A.* 110 (32), 13097–13102.
- Xu, Z., Takizawa, F., Parra, D., Gómez, D., von Gersdorff Jørgensen, L., LaPatra, S.E., Sunyer, J.O., 2016. Mucosal immunoglobulins at respiratory surfaces mark an ancient association that predates the emergence of tetrapods. *Nat. Commun.* 7 (1) (Article 10728).
- Zarkasi, K.Z., Abell, G.C.J., Taylor, R.S., Neuman, C., Hatje, E., Tamplin, M.L., Katouli, M., Bowman, J.P., 2014. Pyrosequencing-based characterization of gastrointestinal bacteria of Atlantic Salmon (*Salmo Salar* L.) within a commercial mariculture system. *J. Appl. Microbiol.* 117 (1), 18–27.
- Zarkasi, K.Z., Taylor, R.S., Abell, G.C.J., Tamplin, M.L., Glencross, B.D., Bowman, J.P., 2016. Atlantic Salmon (*Salmo Salar* L.) gastrointestinal microbial community dynamics in relation to digesta properties and diet. *Microb. Ecol.* 71 (3), 589–603.